

PAPER

Energetically constrained co-tunneling of cold atoms

To cite this article: Andrey R Kolovsky *et al* 2012 *New J. Phys.* **14** 075002

View the [article online](#) for updates and enhancements.

Related content

- [Dissipation-induced hard-core boson gas in an optical lattice](#)
J J García-Ripoll, S Dürr, N Syassen *et al.*
- [Quantum interference-induced stability of repulsively bound pairs of excitations](#)
Lea F Santos and M I Dykman
- [Atomic lattice excitons: from condensates to crystals](#)
A Kantian, A J Daley, P Törmä *et al.*

Recent citations

- [NOON states via a quantum walk of bound particles](#)
Enrico Compagno *et al*
- [Exact quantum decay of an interacting many-particle system: the Calogero–Sutherland model](#)
Adolfo del Campo
- [Escape dynamics of a Bose-Hubbard dimer out of a trap](#)
Dmitrii N. Maksimov and Andrey R. Kolovsky

Energetically constrained co-tunneling of cold atoms

Andrey R Kolovsky^{1,2,4}, Julia Link³ and Sandro Wimberger³

¹ Kirensky Institute of Physics, 660036 Krasnoyarsk, Russia

² Siberian Federal University, 660041 Krasnoyarsk, Russia

³ Institut für Theoretische Physik, Universität Heidelberg,
69120 Heidelberg, Germany

E-mail: andrey.r.kolovsky@gmail.com

New Journal of Physics **14** (2012) 075002 (13pp)

Received 19 January 2012

Published 3 July 2012

Online at <http://www.njp.org/>

doi:10.1088/1367-2630/14/7/075002

Abstract. We study under-barrier tunneling for a pair of energetically bound bosonic atoms in an optical lattice with a barrier. We identify the conditions under which this exotic molecule tunnels as a point particle with the coordinate given by the bound pair center of mass and discuss the atomic co-tunneling beyond this regime. In particular, we quantitatively analyze resonantly enhanced co-tunneling, where two interacting atoms penetrate the barrier with higher probability than a single atom.

Contents

1. Introduction	2
2. Two-state and one-state models	2
3. Under-barrier tunneling for the two-state model	5
4. The full system	7
5. Conclusions	9
Acknowledgments	11
Appendix	11
References	13

⁴ Author to whom any correspondence should be addressed.

1. Introduction

The phenomenon of under-barrier tunneling is one of the most exciting predictions of quantum mechanics, which does not fit the classical picture of the world. As a bright example of a pure quantum effect, it has been considered in all textbooks on quantum mechanics, which might give the impression that under-barrier tunneling has been exhaustively studied already in the early days of quantum mechanics. However, the theoretical description of under-barrier tunneling is simple only for a point particle in one dimension. If we have a composite object, the problem of tunneling becomes very involved. Systematically, this problem was first addressed in nuclear physics (see [1] and references therein). It was found that the tunneling probability for the composite object may considerably differ from that for the point particle of the same mass.

In this work, we revisit the problem of the under-barrier tunneling for a composite object which has become experimentally available only recently—the pair of interacting bosonic atoms in an optical lattice, where two atoms stay close to each other due to an energetic constraint [2]. Note that such atomic pairs exist for both attractive and repulsive inter-atomic interactions if one satisfies the necessary condition that the interaction energy $|U|$ exceeds the single-atom tunneling energy J . Following [2], we shall refer to this exotic two-atom molecule as the bound pair. It admits a simple yet rigorous description [3–6], which greatly facilitates theoretical studies on different aspects of composite object tunneling.

The other motivation for studying the under-barrier tunneling of the bound pair is the problems of many-particle tunneling in correlated systems [7, 8] and macroscopic tunneling of a Bose–Einstein condensate of cold atoms [9–12]. In particular, the recent paper [12] analyzes numerically the under-barrier tunneling of a bright soliton consisting of $N \gg 1$ condensed atoms. Since the bound pair can be considered to be a bright soliton with $N = 2$ atoms [3, 13], a rigorous analysis of the bound-pair tunneling is a first step in the microscopic understanding of macroscopic tunneling.

The structure of this paper is as follows. In section 2, we recall the main results on eigenstates of the bound pair in the absence of an external potential and introduce a simple two-state model, which suffices to describe the mobility of the bound pair. Section 3 is devoted to the under-barrier tunneling within the framework of the two-state model. We identify the conditions under which the bound pair tunnels as a point particle with the coordinate given by the center of mass of the bound pair and uncover the effect of resonant tunneling, which is entirely due to the internal degrees of freedom of the composite object. The main drawback of the two-state model is that it neglects the dissociation process where the barrier breaks the pair into two unbound atoms. For this reason, in section 4 we simulate the tunneling process numerically without using any approximations. We summarize our findings in section 5.

2. Two-state and one-state models

As mentioned in the introduction, the strongly interacting bosons in a lattice form bound pairs, where two bosons occupy the same site. Such a pair can move across the lattice by virtually breaking the bond. At the formal level this is the second-order tunneling, which was experimentally studied in [14]) and, thus, is a composite object with well-defined kinetic energy. The dispersion relation $E(\kappa)$ for the bound pair can be easily calculated numerically by diagonalizing the Hamiltonian of the Bose–Hubbard model (see equation (1)) with $N = 2$ particles. For the purpose of future references, figure 1(a) shows the result of this diagonalization

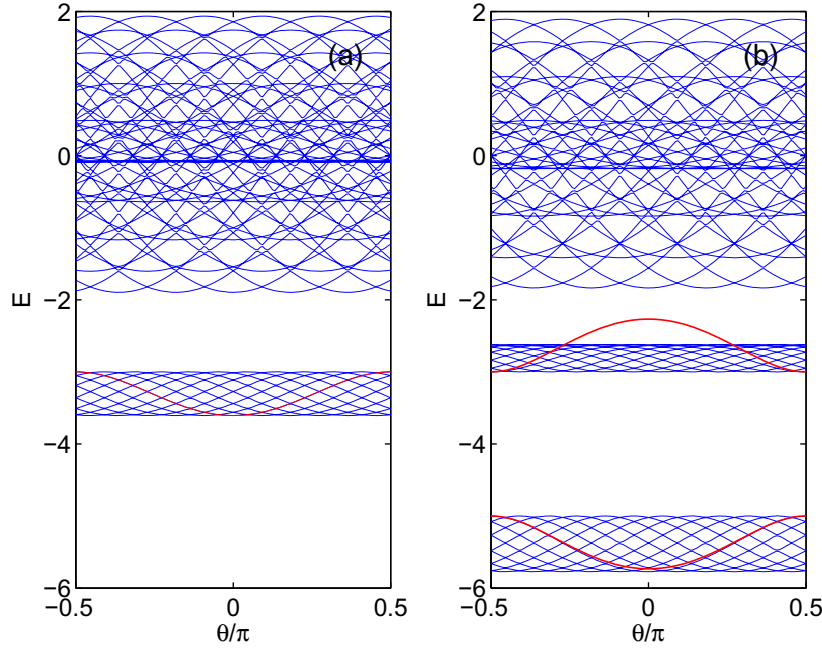


Figure 1. The band spectrum of the system (1) for $J = 1$ and $(U_0, U_1) = -(2, 0)$ (left panel) and $(U_0, U_1) = -(5, 3)$ (right panel). The lattice comprises 11 sites with periodic boundary conditions. The red lines are equation (5) (left panel) and equation (4) (right panel).

for a lattice comprising 11 sites, where we additionally parameterize the Bose–Hubbard Hamiltonian by the Peierls phase θ : $\hat{a}_{l+1}^\dagger \hat{a}_l \rightarrow \hat{a}_{l+1}^\dagger \hat{a}_l \exp(i\theta)$. In figure 1(a) the bound pair of two bosons is associated with the lower band, while the upper band is the spectrum of two hard-core bosons. The problem can also be solved analytically, either exactly or by using a perturbative approach. In the rest of this section we discuss the dispersion relation $E(\kappa)$ and the eigenstates of the bound pair within the perturbative approach, which better fits our aims of studying the tunneling process.

To facilitate the theoretical analysis it is convenient to consider the Bose–Hubbard model which also includes interactions in neighboring sites:

$$\hat{H}_{\text{BH}} = -\frac{J}{2} \sum_l \left(\hat{a}_{l+1}^\dagger \hat{a}_l + \text{h.c.} \right) + \frac{U_0}{2} \sum_l \hat{n}_l (\hat{n}_l - 1) + U_1 \sum_l \hat{n}_{l+1} \hat{n}_l. \quad (1)$$

Inclusion of the latter term explicitly introduces excited states of the bound pair; see figure 1(b). We note that we do not assign the interaction constant U_1 any physical meaning (needless to say, there could be physical cases when $U_1 \neq 0$: see, e.g., [15]): our motivation for introducing the constant U_1 is to separate in the parameter space the process of under-barrier tunneling from the dissociation process which may take place when the bound pair hits the barrier. At the final step of the analysis we let U_1 tend to zero, thus recovering the standard Bose–Hubbard model. The perturbative approach to the energy spectrum of the bound pair essentially amounts to a truncation of the Hilbert space of the operator (1) to the subspace which includes only the Fock states where two bosons occupy either the same site or two neighboring sites. Then, denoting by $\Psi_l^{(1)}$ the probability amplitude to find two bosons at the site l and by $\Psi_l^{(2)}$ the probability

amplitude to find them at sites l and $l + 1$, the eigenvalue equation for the bound pair takes the form $(\widehat{H}_0\Psi)_l = E\Psi_l$, where

$$(\widehat{H}_0\Psi)_l = -\frac{\sqrt{2}J}{2} \left[\begin{pmatrix} 0 & 0 \\ 1 & 0 \end{pmatrix} \Psi_{l-1} + \begin{pmatrix} 0 & 1 \\ 1 & 0 \end{pmatrix} \Psi_l + \begin{pmatrix} 0 & 1 \\ 0 & 0 \end{pmatrix} \Psi_{l+1} \right] + \begin{pmatrix} U_1 & 0 \\ 0 & U_0 \end{pmatrix} \Psi_l. \quad (2)$$

The solutions to this eigenvalue problem are plane waves, $\Psi_l = \mathbf{C}(\kappa)e^{i\kappa l}$, where the vector $\mathbf{C}(\kappa)$ satisfies the following 2×2 eigenvalue equation:

$$\begin{pmatrix} \Delta & -J(1+e^{i\kappa})/\sqrt{2} \\ -J(1+e^{-i\kappa})/\sqrt{2} & 0 \end{pmatrix} \mathbf{C} = E\mathbf{C}, \quad \Delta = |U_0 - U_1|. \quad (3)$$

From (3) we have

$$E(\kappa) = U_0 + \frac{\Delta}{2} \pm \sqrt{\left(\frac{\Delta}{2}\right)^2 + 2J^2 \cos^2\left(\frac{\kappa}{2}\right)}. \quad (4)$$

In what follows, we refer to equations (2)–(4) as the two-state model.

It is worth stressing that the two-state model provides only an approximation to the exact eigenstates of the bound pair. How good this approximation is depends on the system parameters. In general, the two-state model is a good approximation for both the ground and excited bands if $|U_1|, |U_0| \gg J$ and $\Delta \ll |U_1|, |U_0|$. If $|U_1|$ is decreased, yet $|U_0| \gg J$, it is still a reasonable approximation for the ground band (minus sign in equation (4)). This includes the case $U_1 = 0$ where the excited band is ‘dissolved’ into the spectrum of unbound bosons. In this case, according to our numerical analysis, $|U_0|$ should be at least twice as large as J . Then the admixture of the truncated Fock states (i.e. those belonging to the truncated subspace of the Hilbert space) with the exact ground state of the bound pair does not exceed 5%. For smaller $|U_0|$, the contribution of these Fock states cannot be neglected and one has to diagonalize the Hamiltonian (1) in the whole Hilbert space [4], which results in the dispersion relation

$$E(\kappa) = -\sqrt{U_0^2 + 4J^2 \cos^2(\kappa/2)}. \quad (5)$$

In figure 1 we plot the analytical results (5) and (4) by the red lines.

If the band gap $\Delta \gg J$ the problem can be simplified further, resulting in the one-state model. The procedure goes as follows. First we restrict ourselves to the ground band and introduce the Wannier states Φ_l of the bound pair by integrating its translationally invariant eigenstate Ψ_κ over the quasimomentum in the first Brillouin zone:

$$\Phi_l = \int_{-\pi}^{\pi} \Psi_\kappa e^{-i\kappa l} d\kappa = \int_{-\pi}^{\pi} \mathbf{C}^{(-)}(\kappa) e^{i(l-l)\kappa} d\kappa. \quad (6)$$

The Wannier states (6) are localized functions with the center of gravity at the site l . (For example, for $J = 1$, $U_0 = -4$ and $U_1 = 0$ we have $|\Psi_0\rangle \approx 0.157|\dots, 0, 1, 1, 0, 0, \dots\rangle + 0.975|\dots, 0, 0, 2, 0, 0, \dots\rangle + 0.157|\dots, 0, 0, 1, 1, 0, \dots\rangle$.) Next we calculate matrix elements of the Hamiltonian (2) for the Wannier states separated by m sites: $I_m = \langle \Phi_{l+m} | \widehat{H}_0 | \Phi_l \rangle$. This way we obtain the effective Hamiltonian where the bound pair is considered to be a point particle:

$$\widehat{H}_{\text{eff}} = -\frac{1}{2} \sum_m I_m \sum_l \left(\hat{b}_{l+m}^\dagger \hat{b}_l + \text{h.c.} \right). \quad (7)$$

In the limit $\Delta \gg J$ we have $I_1 = 2J^2/\Delta$ and one can safely neglect the next to neighboring hopping. Obviously, this situation corresponds to the case when the dispersion relations (4) and (5) are approximated by the cosine function (which in practice requires $\Delta > 4J$).

3. Under-barrier tunneling for the two-state model

The one-state model (7) introduced in the previous section gives us the reference frame for studying the under-barrier tunneling of the bound pair. To be specific we shall consider a Gaussian barrier, $\epsilon_l = V \exp(-l^2/2\sigma^2)$, and a plane wave coming from minus infinity. Since the Gaussian barrier is well localized within the finite interval $|l| < L \sim \sigma$, we can find the tunneling probability by using, for example, the transfer matrix method (see the [appendix](#)). Alternatively, one finds the tunneling probability by simulating the scattering process for a localized wave packet on the basis of the time-dependent Schrödinger equation:

$$i\partial_t \psi_l = -\frac{1}{2} \sum_m I_m (\psi_{l+m} + \psi_{l-m}) + 2\epsilon_l \psi_l, \quad \epsilon_l = V \exp(-l^2/2\sigma^2). \quad (8)$$

As the initial conditions for (8) it is convenient to choose a wide Gaussian with the given group velocity, $\psi_l(t=0) = G(l-l_0) \exp(i\kappa l)$. If the width of this initial packet is large enough, the result of time-dependent simulations practically coincides with that obtained on the basis of the stationary Schrödinger equation.

A remark concerning the sign of the parameter V is in order. In what follows we consider both positive and negative V , i.e. potential barriers and wells. In fact, for a particle in a lattice the notions of ‘barrier’ and ‘well’ are equivalent to each other to some extent. This becomes especially clear in the case of neighboring hopping ($I_m = I_1 \delta_{m,1}$), where scattering of the plane wave with the quasimomentum κ on the well ($V < 0$) is equivalent to scattering of the plane wave with the quasimomentum $\kappa' = \pi - \kappa$ on the barrier ($V > 0$). (Note that for $\kappa = \pi/2$ this implies a symmetric function $P_t(V)$ for the tunneling probability.) Also, by considering both positive and negative V we cover the case of repulsive interactions as well, with the obvious substitution $V \rightarrow -V$ when the sign of interaction constants is changed.

All remarks above about the one-state model equally apply to the two-state model. Here, instead of (8), one deals with the Schrödinger equation

$$i\partial_t \Psi_l = (\widehat{H}_0 \Psi)_l + \begin{pmatrix} \epsilon_l + \epsilon_{l+1} & 0 \\ 0 & 2\epsilon_l \end{pmatrix} \Psi_l, \quad (9)$$

where Ψ_l is a two-component vector and the Hamiltonian \widehat{H}_0 is defined in equation (2). Our particular interest is in the scattering of a plane wave transmitting in the ground energy band. As an example, figure 2 shows the tunneling probability for the plane wave with $\kappa = \pi/2$ for three different values of the parameter Δ . In panels (b) and (c) of this figure, we have additionally plotted the tunneling probability obtained on the basis of the one-state model.

A remarkable prediction of the two-state model as compared to the one-state model is the appearance of narrow transparency windows for negative V . Usually, such windows are associated with resonant tunneling in multi-barrier structures. In our case (a single barrier or well) we meet a different type of resonant tunneling, where the bound pair tunnels through the upper band or, more precisely, through a localized state of the bound pair in the excited state, as is pictorially shown in figure 3. This interpretation of enhanced tunneling is strongly

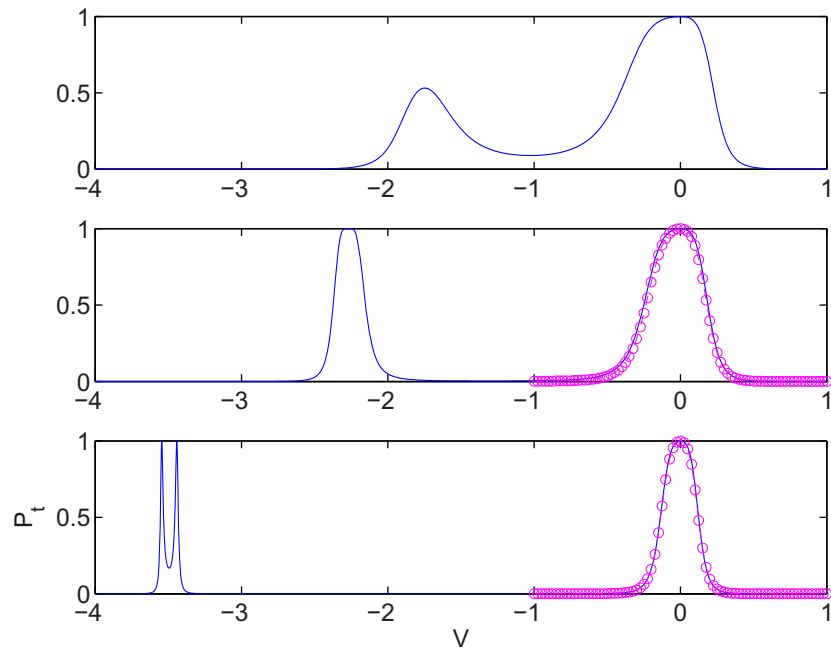


Figure 2. Two-state model: tunneling probability as a function of V for fixed $\kappa = \pi/2$ and $\Delta = 1, 2, 4$ from top to bottom. The scattering potential is $\epsilon_l = V \exp(-l^2/2\sigma^2)$, $\sigma = 0.65$. The open circles are predictions of the one-state model.

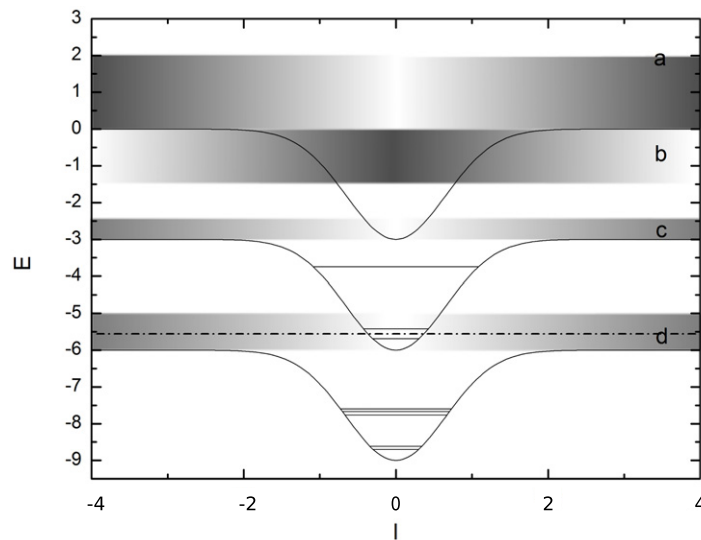


Figure 3. Pictorial representation of the resonant tunneling. Letters ‘d’ and ‘c’ label the ground and excited energy bands of the bound pair; ‘b’ is the energy band of two bosons with one of them captured in the well and ‘a’ is for unbounded bosons.

supported by numerical simulations of the wave-packet dynamics, where we observe a temporal population of the upper band when the packet passes through the well. This is shown by the dashed line in figure 4, where the upper curve is the total occupation probability of Fock states

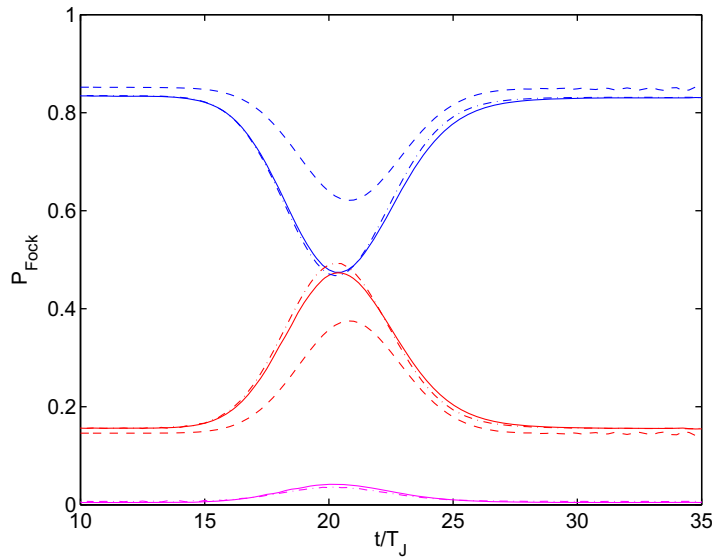


Figure 4. The total occupation probability of Fock states with two bosons in the same site (top curves), Fock states with two bosons in neighboring sites (middle curves) and Fock states with two bosons separated by empty sites (bottom curves). The dashed, dash-dotted and solid lines distinguish between the two-state model, the three-state model (see the discussion at the end of section 4) and the original system. Parameters are $J = 1$, $(U_0, U_1) = -(4, 2)$ (hence $\Delta = 2$), $\sigma = 0.65$ and $V = -2.2$.

with two bosons in the same site and the middle curve is the total occupation probability of Fock states with two bosons in the neighboring sites.

The number and width of resonances seen in $P_t(V)$ crucially depend on the system parameters, in particular, on the width σ of the potential well. If σ is increased, we observe more resonances and they are narrower. The decrease of Δ makes resonances wider. It should also be mentioned that, for the currently considered Gaussian potential, the resonances appear in pairs, as seen in figure 2(c), and the pair can merge into the single wide resonance, as is the case depicted in figures 2(a) and (b).

4. The full system

Next we discuss the degree of validity of the two-state model. Indeed, the two-state model neglects the coupling to the truncated Fock states, which are associated with unbound bosons. If this coupling is strong (as in the case $U_1 \approx 0$, where the upper band of the two-state model is embedded into the energy band of hard-core bosons) it may essentially affect the tunneling process and even open new scattering channels where the bound pair dissociates. For this reason we simulate the tunneling process on the basis of the Bose–Hubbard model (1), i.e. without using any approximations. In this numerical experiment we propagate the wide Gaussian packet constructed from eigenstates of the bound pair for a time approximately two times longer than that required for the packet to hit the potential barrier. Figure 5 shows a typical result for $U_0 = -2$, $U_1 = 0$ and $V = -2$. The figure depicts probabilities of finding the system in the

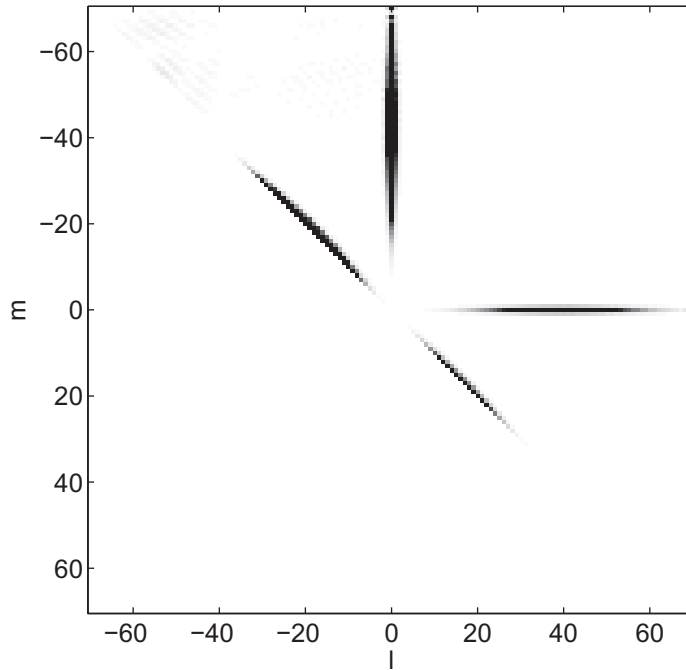


Figure 5. Result of numerical simulations for the wave-packet dynamics of the original system for $J = 1$, $U_0 = -2$, $U_1 = 0$, $\sigma = 0.65$ and $V = -2$. The figure encodes (by using the gray-scaled mapping) the probability of finding two bosons at sites l and m .

Fock state with one boson at the site l and the other one at the site m . (Note that $m \geq l$ in the considered case of identical particles.) It is seen in figure 5 that the initial packet splits into four packets where two of them, which are located at the main diagonal, are associated with the bound pair and the other two are the dissociated pair with one boson staying in the potential well. (For the chosen parameters the dissociation is energetically allowed because the boson in the well accumulates almost the whole bound energy.) Summing up probabilities for these four packets, which are well separated in the Fock space, we find the tunneling, reflection and dissociation probabilities.

To systematically study the effect of the Hilbert space truncation (i.e. the effect of unbound bosons), we fixed the parameter $\Delta = |U_0 - U_1|$ and vary the interaction energy U_1 , where the limiting case corresponds to $U_1 = 0$. The parameter κ , which defines the group velocity of the incoming wave packet, is fixed at $\kappa = \pi/2$ and the parameter σ , which defines the width of the potential barrier, is $\sigma = 0.65$ (then the scattering potential essentially comprises three lattice sites). The results of our numerical simulations are depicted in figure 6 by symbols, which are connected by a dotted line to guide the eyes. Open circles show the tunneling probability and asterisks the dissociation probability. (The reflection probability, which is obviously given by $P_r = 1 - P_t - P_d$, is not shown.) By inspection of the numerical data we can draw the following conclusions: (i) There are practically no deviations from the predictions of the one- and two-state models for the main transparency window around $V = 0$. Thus, here the bound pair tunnels just like a point particle. (ii) The system exhibits resonant tunneling at $V \approx \Delta$, as predicted by the two-state model. This is a clear manifestation of the complex structure of the tunneling

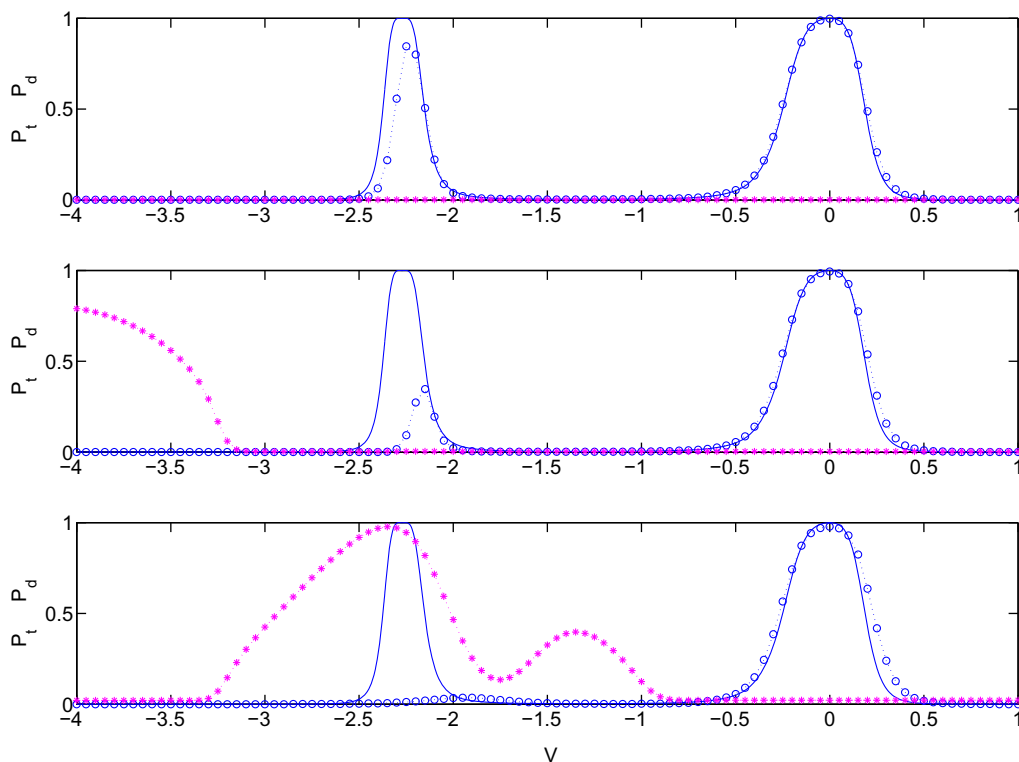


Figure 6. Tunneling (open circles) and dissociation (asterisks) probabilities versus V . The system parameters are $\kappa = \pi/2$, $J = 1$, $\sigma = 0.65$ and $(U_0, U_1) = -(8, 6)$ (top), $-(4, 2)$ (middle), and $-(2, 0)$ (bottom). The solid line is the prediction of the two-state model.

object. (iii) As compared to the two-state model the resonant tunneling is suppressed. It is interesting to note that the tunneling is suppressed independently of whether the dissociation channel is open or closed. (iv) If the dissociation channel is open, we observe strong back action of the resonant tunneling on the dissociation process, which manifests itself in a local deep in $P_d = P_d(V)$.

Let us discuss the suppression of the resonant tunneling in some more detail. We found this suppression to be fairly reproduced if the Hilbert space of the two-state model is enlarged by including the Fock states, where two bosons are separated by one empty site. In other words, instead of the two-state model one considers a three-state model. The dash-dotted lines in figure 4 show population dynamics for the considered three families of Fock states. It is seen that it practically coincides with that for the full system. Note that the third state remains practically unpopulated during the tunneling process. Nevertheless, the presence of this third state appears to be important. This statement is also supported by the transfer matrix analysis, where the inclusion of this state considerably modifies the resonant tunneling (see the [appendix](#)).

5. Conclusions

We studied the tunneling of an interactively bound pair of two bosons in a 1D lattice through a narrow potential barrier/well. This system is, perhaps, the simplest composite object that

can be created in the laboratory. We address the question of under which conditions this composite object tunnels like a point particle. Loosely speaking, these conditions amount to the requirement that the microscopic interaction constant U_0 entering the Bose–Hubbard Hamiltonian is larger than the height of the potential barrier (the case of repulsive interactions) or the depth of the potential well (attractive interactions). If this condition is satisfied, the pair can be considered to be a point particle. Note that the effective Hamiltonian for this ‘point particle’ contains next to neighboring hopping, which is absent in the original Bose–Hubbard Hamiltonian. This takes into account the finite size of our composite object when it is treated as a point object [1, 16].

If the above condition is violated, one meets two phenomena which are entirely due to internal degrees of freedom of the composite object. These are (i) resonant tunneling and (ii) dissociation. Under conditions of resonant tunneling the bound pair can tunnel through the barrier, which the single boson cannot penetrate. (Here we refer to the case of repulsive interactions.) Assuming the shape of the barrier to be fixed, resonant tunneling takes place in a rather small region of the parameter space spanned by the quasimomentum κ of the incoming plane wave (or, equivalently, by the group velocity of the incoming wave packet) and the height V of the potential barrier. In contrast, the parameter region where the external potential breaks the pair by capturing one boson at the barrier is relatively large. For a generic form of the external potential and $U_1 = 0$, the region of resonant tunneling is usually embedded into the dissociation region and, thus, resonant tunneling and dissociation coexist. We observed a strong mutual influence of these processes, which results in a suppression of both tunneling and dissociation.

In the present work we calculated the tunneling and dissociation probabilities by simulating the wave-packet dynamics of the bound pair⁴ where, as the physical object, we had in mind ultra-cold atoms in the 1D optical lattice with the scattering potential created by an additional laser beam crossing the lattice at the right angle. For this reason we considered a Gaussian shape of the potential barrier/well. It seems unlikely that one can obtain a compact analytical expression for the tunneling and dissociation amplitudes for this scattering potential. However, there are good prospects in developing the analytic theory for particular shapes of the barrier/well, which includes the impurity-like potential $\epsilon_l = V\delta_{l,0}$ and the box-like potential $\epsilon_l = V(\delta_{l,0} + \delta_{l,1})$. The advantage of the latter potential is that the well size and the size of the bound pair in the excited state match exactly and, thus, the resonant tunneling and dissociation regions do not overlap.

To conclude the paper, we discuss the relation between our dimensional parameters and parameters of the laboratory experiment [2]. The authors of the cited experiment use the three-dimensional (3D) optical lattice of the depth $V_x = 35$, $V_y = 35$ and $3 < V_z < 10$ in units of the recoil energy defined by the lattice. Large values of V_x and V_y suppress tunneling along the x - and y -directions and, thus, the bound pairs can move only along the z -direction. The ratios of the interaction constant U_0 to the hopping matrix element J are $U_0/J = 15$ for $V_z = 10$ and $U_0/J = 1.5$ for $V_z = 3$, which coincide with the values U_0/J used in our numerical simulations. To study the under-barrier tunneling of bound pairs this setup should be extended by a sheet laser beam [20] normal to the z -axis, which creates a narrow potential barrier, and the pairs should be accelerated to a given quasimomentum κ by applying a static force for a given time, which is a standard technique in experimental studies of atomic Bloch oscillations. These modifications of the experiment [2] would realize our model, but with one important difference. In this paper,

⁴ We mention the papers [17–19] that are also devoted to wave-packet dynamics of the bound pair.

we analyzed the tunneling of a *single* bound pair, while in the laboratory experiment each of the 1D lattices contains several bound pairs. We reserve the problem of sequential tunneling of several bound pairs for future theoretical studies.

Acknowledgments

The present project was supported by the Excellence Initiative (Enable Fund of the Faculty of Physics and Astronomy, Heidelberg University). Moreover, SW acknowledges financial support from the DFG through FOR760, the Helmholtz Alliance Program of the Helmholtz Association (contract number HA-216: Extremes of density and temperature: cosmic matter in the laboratory), and by the Heidelberg Graduate School of Fundamental Physics (grant number GSC 129/1) and AK acknowledges support from the Russian Foundation for Basic Research (project number 12-02-000094-a: Tunneling of the macroscopic quantum states) and by the Siberian Branch of RAS (project no. 29: Dynamics of atomic Bose–Einstein condensates in optical lattices). AK is very grateful for the hospitality of the Institute of Theoretical Physics of Heidelberg University.

Appendix

The transfer matrix propagates the plane wave solution $\psi_l = \exp(i\kappa l)$ from the asymptotic region $l < -L$ to the asymptotic region $l > L$, where the wave function is given by the superposition of two plane waves, $\psi_l = a \exp(-i\kappa l) + b \exp(i\kappa l)$. Then the tunneling amplitude is given by $t = 1/b^*$. This relation is valid independently of whether the wave function is scalar or vector, although the explicit form of the transfer matrix is different.

We begin with the one-state model (7) where we assume $I_m = I\delta_{m,1}$ for simplicity:

$$-\frac{I}{2}(\psi_{l+1} + \psi_{l-1}) + 2\epsilon_l \psi_l = E \psi_l, \quad E(\kappa) = -I \cos \kappa. \quad (\text{A.1})$$

It immediately follows from (A.1) that the plane wave can be propagated as

$$\begin{pmatrix} \psi_{l+1} \\ \psi_l \end{pmatrix} = T_l \begin{pmatrix} \psi_l \\ \psi_{l-1} \end{pmatrix}, \quad (\text{A.2})$$

where

$$T_l = \begin{pmatrix} 2(2\epsilon_l - E)/I & -1 \\ 1 & 0 \end{pmatrix} \quad (\text{A.3})$$

is the one-step transfer matrix. It is worth noting that the matrix (A.3) is unitary, with the eigenvalues lying on the unit circle.

The case of the two-state model is more involved. Here equation (A.2) takes the form

$$\begin{pmatrix} \Psi_{l+1}^{(2)} \\ \Psi_{l+1}^{(1)} \end{pmatrix} = T_l \begin{pmatrix} \Psi_l^{(2)} \\ \Psi_l^{(1)} \end{pmatrix} \quad (\text{A.4})$$

and the transfer matrix is given by

$$T_l = \begin{pmatrix} (ab - 1) & -b \\ a & -1 \end{pmatrix}, \quad (\text{A.5})$$

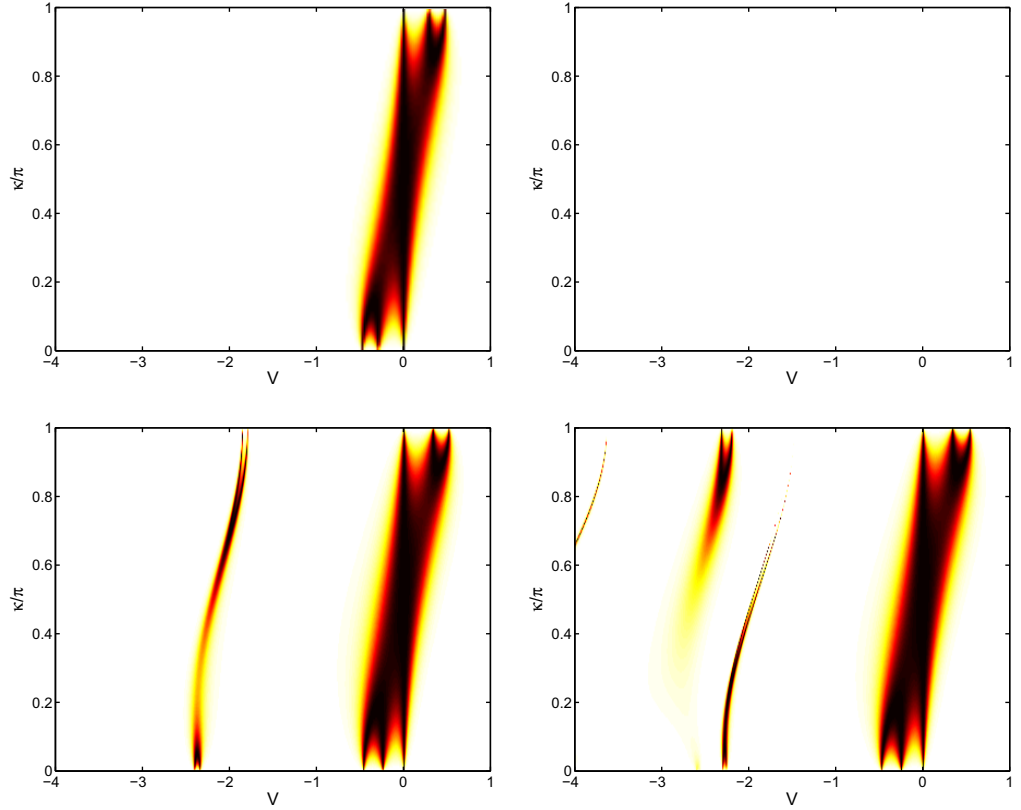


Figure A.1. Tunneling probability as predicted by the one-state (upper left), two-state (upper right) and three-state (lower row) models. The system parameters are $J = 1$, $\Delta = 2$ and $U_1 = -2$ in the lower left panel and $U_1 = 0$ in the lower right panel; the width of the Gaussian scattering potential $\sigma = 0.65$.

where $a = \sqrt{2}(\Delta + \epsilon_l + \epsilon_{l+1} - E)/J$ and $b = \sqrt{2}(2\epsilon_{l+1} - E)/J$. The dispersion relation $E = E(\kappa)$ entering equation (A.5) is obtained by solving the Schrödinger equation in the absence of the scattering potential and is given in equation (4).

Finally, we display the transfer matrix for the three-state model. It has the most compact form if we propagate the column vector $(\Psi_l^{(2)}, \Psi_l^{(1)}, \Psi_{l-1}^{(3)})^T$ with the shifted index for the third component. Then the transfer matrix is given by

$$T_l = A^{-1}B, \quad (\text{A.6})$$

where the matrices A and B are as written below:

$$A = \begin{pmatrix} -1/\sqrt{2} & (U_0 + 2\epsilon_{l+1} - E)/J & 0 \\ -1/2 & 0 & (\epsilon_l + \epsilon_{l+2} - E)/J \\ 0 & -1/\sqrt{2} & -1/2 \end{pmatrix} \quad (\text{A.7})$$

and

$$B = \begin{pmatrix} 1/\sqrt{2} & 0 & 0 \\ 1/2 & 0 & 0 \\ (E - U_1 - \epsilon_l - \epsilon_{l+1})/J & 1/\sqrt{2} & 1/2 \end{pmatrix}. \quad (\text{A.8})$$

In this paper, when discussing the tunneling probability, we focused on the particular case $\kappa = \pi/2$ where the bound pair has the maximum group velocity. It is interesting to compare the results of the one-, two- and three-state models for other values of the quasimomentum. This comparison is given in figure A.1, which shows the tunneling probability as a function of the quasimomentum κ and the amplitude V of the external Gaussian potential ($\sigma = 0.65$). The system parameters are $J = 1$ and $U_0 = U_1 - 2$, which implies $\Delta = 2$ in the two-state model and $I \approx 0.5$ in the one-state model. (In figure A.1(a) we used $I = 0.7321/2$, which is one half of the actual band width.) A narrow window of the resonant tunneling (as predicted by the two-state model) and partial suppression of this resonant tunneling (as predicted by the three-state model) are clearly seen in the figure.

References

- [1] Zakhariev B N 1996 *Lessons of Quantum Intuition* (Dubna: Joint Institute for Nuclear Research) (in Russian)
- [2] Winkler K, Thalhammer G, Lang F, Grimm R, Hecker Denschlag J, Daley A J, Kantian A, Büchler H P and Zoller P 2006 Repulsively bound atom pairs in an optical lattice *Nature* **441** 853
- [3] Scott A C, Eilbeck J C and Gilhoj H 1994 Quantum lattice solitons *Physica D* **78** 194
- [4] Valiente M and Petrosyan D 2008 Two-particle states in the Hubbard model *J. Phys. B: At. Mol. Opt. Phys.* **41** 161002
- [5] Nygaard N, Piil R and Molmer K 2008 Feshbach molecules in a one-dimensional optical lattice *Phys. Rev. A* **77** 021601
- [6] Javanainen J, Odong O and Sanders J C 2010 Dimer of two bosons in a one-dimensional optical lattice *Phys. Rev. A* **81** 043609
- [7] del Campo A 2011 Long-time behavior of many-particle quantum decay *Phys. Rev. A* **84** 012113
- [8] Pons M, Sokolovski D and del Campo A 2011 Fidelity of fermionic atom-number states subjected to tunneling decay arXiv:1111.1346v1
- [9] Albiez M, Gati R, Fölling J, Hunsmann S, Cristiani M and Oberthaler M K 2005 Direct observation of tunneling and nonlinear self-trapping in a single bosonic Josephson junction *Phys. Rev. Lett.* **95** 010402
- [10] Paul T, Hartung M, Richter K and Schlagheck P 2007 Nonlinear transport of Bose–Einstein condensates through mesoscopic waveguides *Phys. Rev. A* **76** 063605
- [11] Dekel G, Farberovich V, Fleurov V and Soffer A 2010 Dynamics of macroscopic tunneling in elongated Bose–Einstein condensates *Phys. Rev. A* **81** 063638
- [12] Glick J A and Carr L D 2011 Macroscopic quantum tunneling of solitons in Bose–Einstein condensates arXiv:1105.5164
- [13] Flach S and Gorbach A V 2008 Discrete breathers—advances in theory and applications *Phys. Rep.* **467** 1
- [14] Fölling S, Trotzky S, Cheinet P, Feld M, Saers R, Widera A, Müller T and Bloch I 2007 Direct observation of second-order atom tunneling *Nature* **448** 1029
- [15] Wang Y-M and Liang J-Q 2010 Repulsive bound-atom pairs in an optical lattice with two-body interaction of nearest neighbors *Phys. Rev. A* **81** 045601
- [16] Sokolov S N and Zakhariev B N 1964 *Ann. Phys.* **14** 229
- [17] Kudo K, Boness T and Monteiro T S 2009 Control of bound-pair transport by periodic driving *Phys. Rev. A* **80** 063409
- [18] Krimer D O, Khomeriki R and Flach S 2011 Two interacting particles in a random potential *JETP Lett.* **94** 406
- [19] Albrecht C and Wimberger S 2012 Induced delocalization by correlation and interaction in the one-dimensional Anderson model *Phys. Rev. B* **85** 045107
- [20] Ramanathan A, Wright K C, Muniz S R, Zelan M, Hill W T III, Lobb C J, Helmerson K, Phillips W D and Campbell G K 2011 Superflow in a toroidal Bose–Einstein condensate: an atom circuit with a tunable weak link *Phys. Rev. Lett.* **106** 130401